Cellulose (2020) 27:10047–10060
https://doi.org/10.1007/s10570-020-03453-7

ORIGINAL RESEARCH

Tightly-coated and easily recyclable Ag@AgBr-cotton hybrid photocatalyst for organic dye degradation under visible light

Minglei Wang · Maojiang Zhang · Qianhong Gao · Yinjie Liu · Mingxing Zhang · Rongfang Shen · Yumei Zhang · Jiangtao Hu · Guozhong Wu

Received: 8 November 2019 / Accepted: 10 September 2020 / Published online: 26 September 2020

Abstract Immobilization of photocatalysts on substrates is an important factor for water purification in practical applications. In this study, an efficient Ag@AgBr photocatalytic coating was attached onto the surface of cotton fabric via radiation-induced graft polymerization and subsequent chemical reactions, and the resultant product was denoted as Cot-Ag@AgBr. The graft chains acted not only as a source of bromine, but also as an intermediate layer to anchor the Ag@AgBr photocatalytic coating via strong electrostatic interactions. The immobilized Ag@AgBr photocatalytic coating exhibited outstanding photocatalytic properties for organic dye degradation under visible light irradiation. Furthermore, Cot-Ag@AgBr presented high stability and robust durability, which conferred its excellent visible-light-driven photocatalytic activity after five rounds of photodegradation. After 10 min of ultrasonication, the amount of Ag@AgBr precipitate that leached from the Cot-Ag@AgBr was $< 2\%$. Therefore, the as-synthesized cotton fabric offered good insight into the functionalization of polymer substrates with photocatalysts and could be useful for advanced wastewater treatment under the cyclic operations.

Keywords Radiation-induced grafted polymerization · Ag@AgBr · Photodegradation · Durability

M. Wang · M. Zhang · Y. Liu · M. Zhang · R. Shen · J. Hu (✉) · G. Wu (✉)
CAS Center for Excellence on TMSR Energy System, Shanghai Institute of Applied Physics, Chinese Academy of Sciences, No. 2019 Jialuo Road, Jiading District, Shanghai 201800, People's Republic of China
e-mail: hujiangtao@sinap.ac.cn

G. Wu
e-mail: wuguozhong@sinap.ac.cn

M. Wang · M. Zhang
University of Chinese Academy of Sciences, Beijing 100049, People's Republic of China

M. Zhang · G. Wu
School of Physical Science and Technology, ShanghaiTech University, Shanghai 200031, People's Republic of China

Q. Gao
School of Environmental and Biological Engineering, Nanjing University of Science and Technology, 200 Xiaolingwei, Nanjing 210094, Jiangsu Province, People's Republic of China

Y. Zhang
State Key Laboratory for Modification of Chemical Fibers and Polymer Materials, Donghua University, Songjiang, People's Republic of China

Introduction

Water pollution, driven by worsening of the climate, rapid population growth, industrialization and other factors, represents a great threat for the ecological environment and human development (Li et al. 2017). Various technologies and methods, including absorption (Liu et al. 2019), oxidation (Duan et al. 2018), filtration (Nakamura et al. 2019), and biodegradation (Briones et al. 2018) have been used to address these emergent concerns. However, it is difficult to achieve the complete degradation of most refractory organic pollutants, and the current methods cannot meet the emission standards. Developing new technologies has become a global concern for the removal of recalcitrant organic pollutants. Because it is an energy-saving, eco-friendly, and low-cost procedure, photocatalysis is considered to be one of the most promising technologies that uses solar energy for wastewater treatment (Li et al. 2019a, c; Mou et al. 2018). Specifically, TiO_2-based semiconductor photocatalysts have been extensively studied owing to their chemical stability and non-toxicity (Dong et al. 2017; Ma et al. 2019). Nevertheless, TiO_2 presents some inherent disadvantages, such as fast electron–hole recombination rate, low charge separation efficiency, and most importantly, its wide band gap (3.2 eV), which requires ultraviolet light (5% of the solar radiation spectrum) activation. Thus, it is urgent to develop new photocatalysts that make full use of solar energy, particularly the visible light region.

As an excellent photocatalyst, silver bromide (AgBr) has attracted significant attention recently (Huang et al. 2019; Liang et al. 2019; Xu et al. 2019; Zhu et al. 2019). In addition, to further improve the utilization of sunlight, Ag nanoparticles (NPs) were in situ deposited on the surface of AgBr to form the Ag@AgBr heterostructure (Song et al. 2014; Wang et al. 2012; Xiao et al. 2015). Ag NPs with high absorption of visible light resulting in the localized surface plasmon resonance (LSPR) contribute greatly on the photocatalytic activity of AgBr under visible-light irradiation. Additionally, Ag NPs would significantly facilitate the separation of the photoinduced electrons and holes by trapping electrons, and consequently increasing the photocatalytic efficiency of Ag@AgBr. Furthermore, Ag NPs could also improve the stability of AgBr. Typically AgBr NPs is in form of NPs. There are still several drawbacks that limit the practical application of AgBr crystals, such as the utilization of the photocatalysts recycled from the water treatment systems and easy agglomeration of crystals decreasing their catalytic activity. A variety of strategies, such as self-assembly technique (Li et al. 2019b), hydrothermal method (Tan et al. 2013), or use of composite catalysts (L. Chen et al. 2015), have been developed to overcome the aforementioned limitations. Of such strategies, the immobilization of these photocatalytic materials onto supports to obtain large scale catalysts appears to be a feasible protocol. Some formulated hybrids, such as Ag/AgBr-graphene oxide, Ag@AgBr/$BiPO_4$/r-GO, Bi_2MoO_6/Ag/AgCl, Bi_2O_2(-OH)(NO_3)-Br-AgBr and Ag/AgBr-C_3N_4 exhibited high photocatalytic degradation efficiency for pollutants elimination (Fan et al. 2015; Ding et al. 2018a, b; Yang et al. 2019; Zhang et al. 2019a, b; Xu et al. 2013). However, most of the previous studies generally aimed to anchor AgBr crystals onto nano- and micro-scale substrates. Although the obtained composite catalysts could combine the advantages derived from immobilization on small supports and excellent photocatalytic performance of AgBr crystals for water purification under visible light irradiation, recycling these catalysts from aqueous-based media is still a challenge that needs to be addressed. Commercial large cellulose fiber substrates with characteristics of fabrication convenience, simple recyclability, stable reusability, and easy surface modification appear to be the most attractive supports. However, the other limitation for the large-scale preparation of catalysts, namely the attachment between the functional layers and supports, is an important factor that cannot be ignored. Hence, if nanoscale catalysts can be in situ grown on large supports with robust binding force, the resultant products can not only address the recovery concern but also maintain the merits of nanoscale functionalities for reactions (Li et al. 2014; Zhang et al. 2015a, b; Ding et al. 2018a, b; Zhang et al. 2019a, b; Fan et al. 2019).

In this study, Ag@AgBr nanocrystals were in situ deposited onto the surface of commercially available cotton fabric via the radiation-induced graft copolymerization (RIGP) of 2-(dimethylamino) ethyl methacrylate (DMAEMA) followed by self-assembling synthesis. The graft chains were protonated using hydrobromic acid, and then the protonated grafted chain acted as bromine source to directly react with Ag^+ and produce AgBr, which would

homogeneously distribute on the surface of modified cotton. Owing to the instability of silver bromide, the Ag^+ ions in AgBr could be reduced to Ag NPs under visible light irradiation, which would improve the photocatalytic efficiency and stability of AgBr nanocrystals. Further investigations indicated that the graft chains improved the attachment between the cotton fabric and AgBr nanocrystals. The morphology and structure of Ag@AgBr photocatalytic coating attached onto the surface of cotton fabric (Cot-Ag@AgBr) were systematically analyzed using scanning electron microscopy (SEM), X-ray diffraction (XRD), and X-ray photoelectron spectrophotometry (XPS), and the results demonstrated that the Ag@AgBr NPs were successfully anchored onto the surface of cotton. The photocatalytic efficiency of Cot-Ag@AgBr for rhodamine B (RhB) under visible light irradiation arrives at 97% and the degradation rate still reached 89% after five consecutive cycles. Base on electron paramagnetic resonance (EPR) analysis, it was confirmed that the photodegradation of RhB was dominated by the superoxide radicals ($\cdot O_2^-$). This method could be used to prepare functional materials under mild conditions, which opened the possibility of designing new materials. The preparation process was fully compatible with the conventional dyeing and finishing of fabrics, thus it could be very promising for large-scale batch and roll-to-roll preparation of AgBr nanocrystal-coated catalytic materials in the future.

Experimental section

Raw materials

Cotton fabrics (yarn count: 60 × 60, density: 90 × 88, weight: 95 g/m^2, plain weave) were purchased from Kunshan Zhongtian Textile Co., Ltd. (China). DMAEMA, and 5, 5-dimethyl-1-pyrroline N-oxide (DMPO) were purchased from Aladdin Industrial Corporation (China). Acetone (AR), methanol (AR), silver nitrate (AR), and hydrobromic acid (AR) were obtained from Sinopharm Chemical Reagent Co., Ltd. (China). All reactants were used as received.

Preparation of Cot-Ag@AgBr

For organic materials, radiation grafting is an effective and facile way to change its surface properties. Generally, the radiation grafting process includes two steps: (1) the "grafting to", residual free radical of the oligomer can graft to the surface of cotton. However, the grafted chains hinder the approach of oligomer to the surface. (2) the "grafting from", The active site can be produced on the surface of cotton to initiate monomer polymerization (Hu et al. 2016; Qin et al. 2004). Before grafting, the pristine cotton fabric was rinsed with ethanol to remove any organic pollutants from its surface. Scheme 1 illustrates the fabrication process of poly(2-(dimethylamino) ethyl methacrylate) grafted on cotton fabric (Cot-*g*-PDMAEMA) via simultaneous radiation induced grafted polymerization. First, a piece of cotton fabric (10 × 10 cm) was immersed into an irradiation tube that contained methanol solution of DMAEMA monomer (25 vol.%). Then, the solution was injected with nitrogen for 15 min to eliminate the dissolved oxygen. Subsequently, the irradiation tube was sealed and exposed to ^{60}Co γ-rays for 17 h with a total absorbed dose of 10 kGy. Afterwards, the grafted cotton fabrics were cleaned with boiling acetone in a Soxhlet apparatus for 12 h to remove the residual monomer and homopolymer, and finally, the grafted sample was dried in a vacuum oven at 60 °C. The degree of grafting (D_g) was determined based on the following equation:

$$D_g(\%) = (W_1 - W_0)/W_0 \times 100\% \quad (1)$$

where W_0 and W_1 represent the weights of cotton and Cot-*g*-PDMAEMA, respectively, and the D_g of the samples used in this study was was determined to be 45.4%.

The obtained Cot-*g*-PDMAEMA samples were immersed into 0.5% HBr aqueous solution (200 mL) for 2 h at ambient temperature to protonate Cot-*g*-PDMAEMA, leading to the introduction of bromine sources. The resultant samples were rinsed with deionized water for three times to eliminate the excess HBr and then were dried in vacuum. Subsequently, 100 mL $AgNO_3$ (5 mg/mL) was added dropwise into a beaker that contained 200 mL distilled water and the protonated samples under vigorous stirring for 2 h. The resultant samples were ultrasonically cleaned at ambient temperature to peel off the AgBr nanocrystals that were not chemically anchored to the cotton fabric; the resultant material was denoted as Cot-AgBr. To improve the activity and stability of the AgBr nanocrystals, the Cot-AgBr was illuminated for

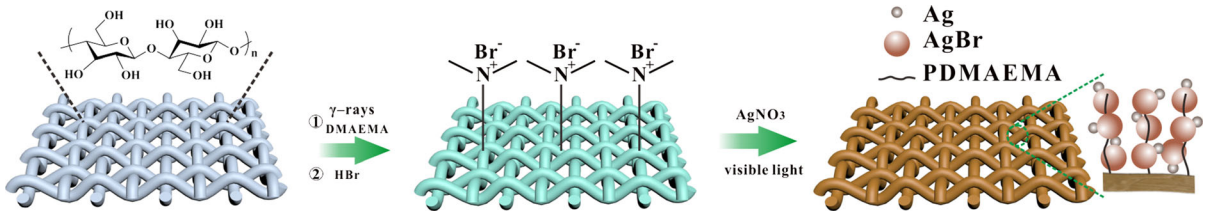

Scheme 1 Schematic illustration of preparation process of Cot-Ag@AgBr

30 min in the presence of ethanol solution using a 350 W Xe lamp to produce Ag NPs. The load of elemental Ag was determined to be 1.7% using inductively coupled plasma atomic emission spectroscopy (ICP-AES), and the obtained material was denoted as Cot-Ag@AgBr.

Measurements

The surface morphology of Cot-Ag@AgBr was observed using a Merlin Compact SEM (Zeiss) instrument. Attenuated total reflection infrared spectra were recorded by using a Tensor 27 spectrometer (Bruker Co., USA) spectrometer in the range of 4000–400 cm^{-1} at the resolution of 4 cm^{-1}. The XRD patterns were obtained using a D/MAX2200 XRD (Rigaku) instrument with Cu Kα radiation. A PHI-5702 XPS(Manufacturer, Country) device with Al Kα radiation was used to analyze the element composition of the samples. The loading amount of Ag@AgBr and Ag leaching during the photocatalytic process were detected using an Optima 8000 ICP-AES (Perkin Elmer) apparatus. Ultraviolet–visible (UV–vis) absorption spectra were recorded using a Ruili 1100 spectrophotometer (Cary 50, USA) spectrophotometer. The KO-100DE sonicator (100 W) with frequency of 40 kHz was used to evaluated the adhesion of Ag@AgBr on the surface of cotton fabric.

Active species detection experiments

The EPR spectra of the prepared Cot-Ag@AgBr samples were measured using a JES-FA200 (Manufacturer, Country) X-band spectrometer with the 100-kHz modulation frequency to analyze the presence of reactive oxygen species (ROS) during the photocatalytic process. We used DMPO as spin trap. In detail, 15 μL of DMPO was added to 0.5 mL aqueous solution or ethanol solution. A piece of synthesized cotton was immersed in the corresponding solution and was then irradiated with a 350 W Xe lamp for 5 min.

Evaluation of photocatalytic activity

In a typical experiment, a 5 × 5 cm piece of Cot-Ag@AgBr was added to 100 mL RhB dye (10 mg/L) aqueous solution in the dark for 30 min to reach the adsorption–desorption equilibrium. Then, the dye solution that contained Cot-Ag@AgBr was irradiated using a 350 W Xe lamp with a cut filter (> 420 nm). After a definite time interval, 1 mL aliquots were collected from the RhB dye solution and were analyzed to determine the remaining concentration of RhB using a U-3010 (Hitachi, Japan) UV–vis spectrophotometer at 553 nm. The degradation percentage was calculated using the formula: C/C_0, where C_0 and C are the initial concentration of RhB after the adsorption equilibrium and the concentration of RhB at the real-time. For comparison, Ag@ZnO and Ag@AgBr powders were employed as references of photocatalysts. The photocatalytic tests under solar light illumination was performed at July 31, 2019 at Shanghai city with a temperature range of 29–36 °C.

Durability evaluation

To evaluate the durability of Cot-Ag@AgBr, a piece of Cot-Ag@AgBr was ultrasonicated in water for a preset time interval. The resultant Cot-Ag@AgBr fabric was rinsed with water and dried under vacuum overnight at 60 °C. Afterward, SEM was employed to observe the changes in surface morphology after ultrasonication. To determine the amount of Ag^+ ions leached from the Cot-Ag@AgBr fabric after the degradation reaction, the reaction mixtures were investigated by ICP-AES.

Results and discussion

Design of Cot-Ag@AgBr

Cotton fabric, as a cheap, washable, renewable, and biodegradable cellulosic material, has been widely used to anchor the photocatalysts (Cheng et al. 2017; Qin et al. 2019; Ran et al. 2019; Wang et al. 2017). However, the surfaces of cotton fabrics are usually smooth, which decreases the strength of the interface bonds between the catalyst and the substrate. Consequently, these macroscale substrates should be surface-functionalized to bind inorganic catalyst precursors and grow them via layer-by-layer self-assembly technology. Conventional methods, such as chemical etching, chemical adhesives, surface-initiated atom-transfer radical polymerization, UV, and plasma-induced polymerization have been extensively studied (Yang et al. 2017; Zhang et al. 2015a, b). However, these processes that are used to modify the characteristics of polymer surfaces still suffer from many difficulties in practical fabrication, such as complicated protocols and devices, limited effect, utilization of environmentally unfriendly precursors, and difficulty in large-scale production. The development of a green and efficient method for attaching photocatalysts onto the surface of substrates while simultaneously achieving strong interfacial bonding and excellent photocatalytic stability is still a formidable challenge. According to previous studies from other researchers and our group (Gao et al. 2016; Jiangtao Hu et al. 2018; Hu et al. 2016; Wang and Zhang 2019; Zhang et al. 2017), simultaneous RIGP can effectively modify the surface characteristics of organic substrates. Therefore, we designed a scheme to address the aforementioned problems. A commercial reagent, the DMAEMA monomer, was grafted onto cotton under γ-ray irradiation. Radicals were generated on the organic supports and in the monomeric solution, which subsequently initiated the polymerization of monomers to facilitate the molecular level covalent bonding between the functional graft chains and cotton fabric during graft polymerization. Afterward, the graft chains reacted with the photocatalyst precursors to introduce photocatalyst seeds onto the cotton substrate. Finally, when the modified cotton was immersed in $AgNO_3$ solution, the surface bromine sources initiated the subsequent growth of the photocatalyst. The preparation process of Cot-Ag@AgBr is illustrated in Scheme 1. This proposed process was conducive for the in situ growth of semiconductor nanocrystals on the surface of substrates with a high durability. For example, the in situ covalent loading of Ag@ZnO NPs onto the surface of cotton fabric via radiation-induced grafting polymerization has been successfully performed in one of our previous studies, which exhibited excellent photocorrosion resistance, catalytic stability, and laundering durability (Wang and Zhang 2019).

Structural characterization of modified fabrics

The surface morphology of the pristine and modified cotton fabrics was observed using SEM. The surface of the pristine cotton fabric was very smooth and clean (Fig. 1a), that of Cot-*g*-PDMAEMA was slightly rough with a gel-like layer (Fig. 1b), which was attributed to the accumulation of graft chains. After protonation, no remarkable changes were observed in the surface morphology of Cot-*g*-PDMAEMA, which indicated that protonation did not affect the sample negatively. Compared with the pristine cotton fabric and the other modified fabrics, Cot-Ag@AgBr was very rough. Specifically, the surface of Cot-Ag@AgBr presented a few dot-shaped Ag/AgBr particles (Fig. 1d), which agglomerated into a thin-layered structure and evenly coated the surface of the fibers.

Figure 2a depicts the FTIR spectra of the pristine cotton fabric, Cot-*g*-PDMAEMA, Cot-HBr, and Cot-Ag@AgBr. Compare with the pristine cotton fabric, a new peak was appeared at 1740 cm^{-1} owing to the presence of –C=O group induced by the grafting of DMAEMA on the surface of the fabric (Zhang et al. 2014). Subsequently, XRD was applied to characterize the crystal structure of the fibers. As illustrated in Fig. 2b, the position and shapes of the diffraction peaks in the spectra of the pristine and modified cotton fabrics were almost the same. This indicated that the crystal structure was not changed during the modification process. With a careful observation, an inconspicuous diffraction peak at 20.5° appeared in the spectra of Cot-*g*-PDMAEMA, Cot-HBr, and Cot-Ag@AgBr, which could be ascribed to the somewhat more random orientation of the crystallites (French 2013; Segal et al. 1959). After the in situ deposition of the Ag@AgBr nanocrystals, series of distinct diffraction peaks of AgBr were observed at the 2θ values of 26.7° (111), 31.0° (200), 44.4° (220), 55.1° (222),

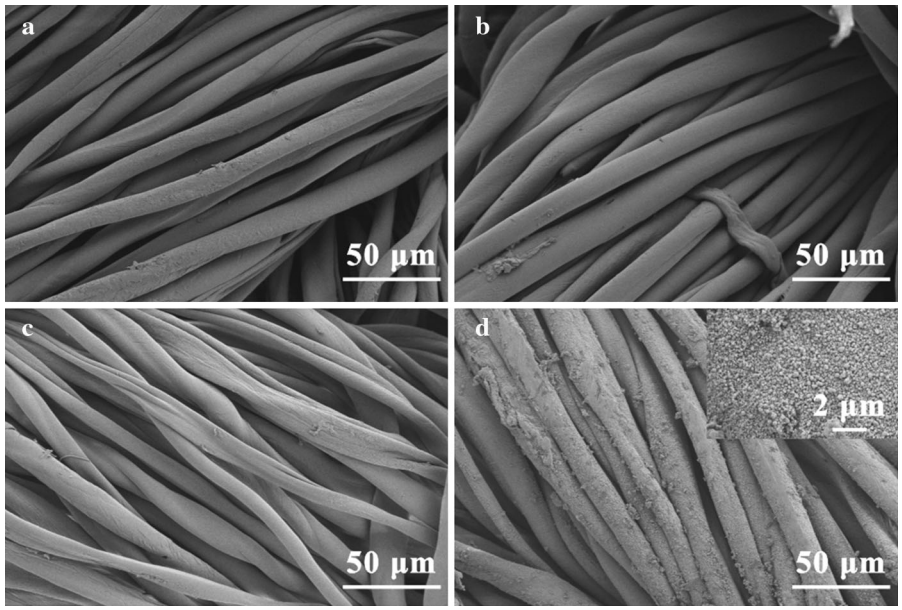

Fig. 1 Scanning electron microscopy images of **a** pristine cotton fabric, **b** poly(2-(dimethylamino) ethyl methacrylate) grafted on cotton fabric (Cot-*g*-PDMAEMA), **c** HBr attached onto cotton fabric (Cot-HBr), and **d** Ag@AgBr attached onto cotton fabric (Cot-Ag@AgBr)

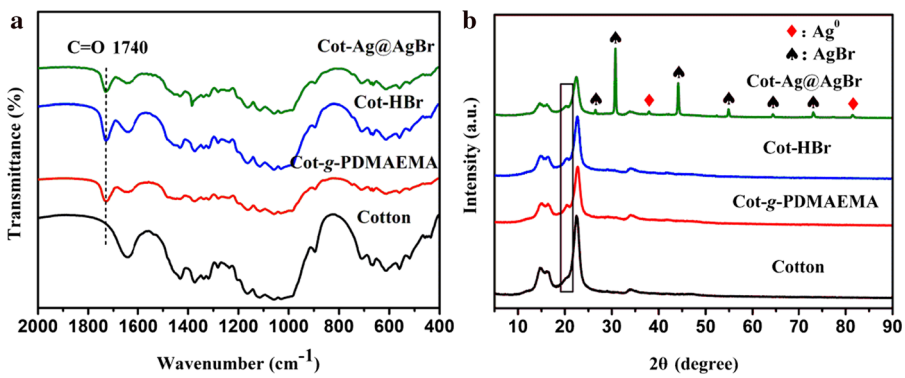

Fig. 2 **a** FT-IR spectra of pristine cotton fabric, Cot-*g*-PDMAEMA, Cot-HBr, and Cot-Ag@AgBr. **b** XRD pattern of pristine cotton fabric, Cot-*g*-PDMAEMA, Cot-HBr, and Cot-Ag@AgBr

64.5° (400), and 73.2° (420) (JCPDS Card No. 79-0149) (Wang et al. 2012). In addition, the diffraction peaks of metallic Ag at 2θ of 38.1° (111) and 81.5° (222) were also identified in the spectrum of Cot-Ag@AgBr, which fitted well with the reported data list for JCPDS Card No. 01-1167, indicating that the presence of Ag NPs derived from the reduction of AgBr under visible light irradiation (Xiao et al. 2015).

The surface chemical composition of the pristine and modified cotton fabrics was further determined using XPS. The wide-scan spectra of the pristine cotton fabric, Cot-*g*-PDMAEMA, Cot-HBr, and Cot-Ag@AgBr are depicted in Fig. 3a. Five elements: C, O, N, Ag, and Br were detected on the surface of Cot-Ag@AgBr, while only C and O elements were identified on the pristine cotton fabric. An additional N 1 s peak that belonged to the -$N(CH_3)_2$ group was detected in the spectrum of Cot-*g*-PDMAEMA, which suggested the successful grafting of PDMAEMA molecules onto the surface of the cotton fabric via covalent bonds. After protonation (Fig. 3b), the N 1s peak split into two peaks: –$N(CH_3)_2$ and –$N^+(CH_3)_2$, and the intensity of –$N^+(CH_3)_2$ was higher than that of -$N(CH_3)_2$ owing to the conversion of -$N(CH_3)_2$ to –

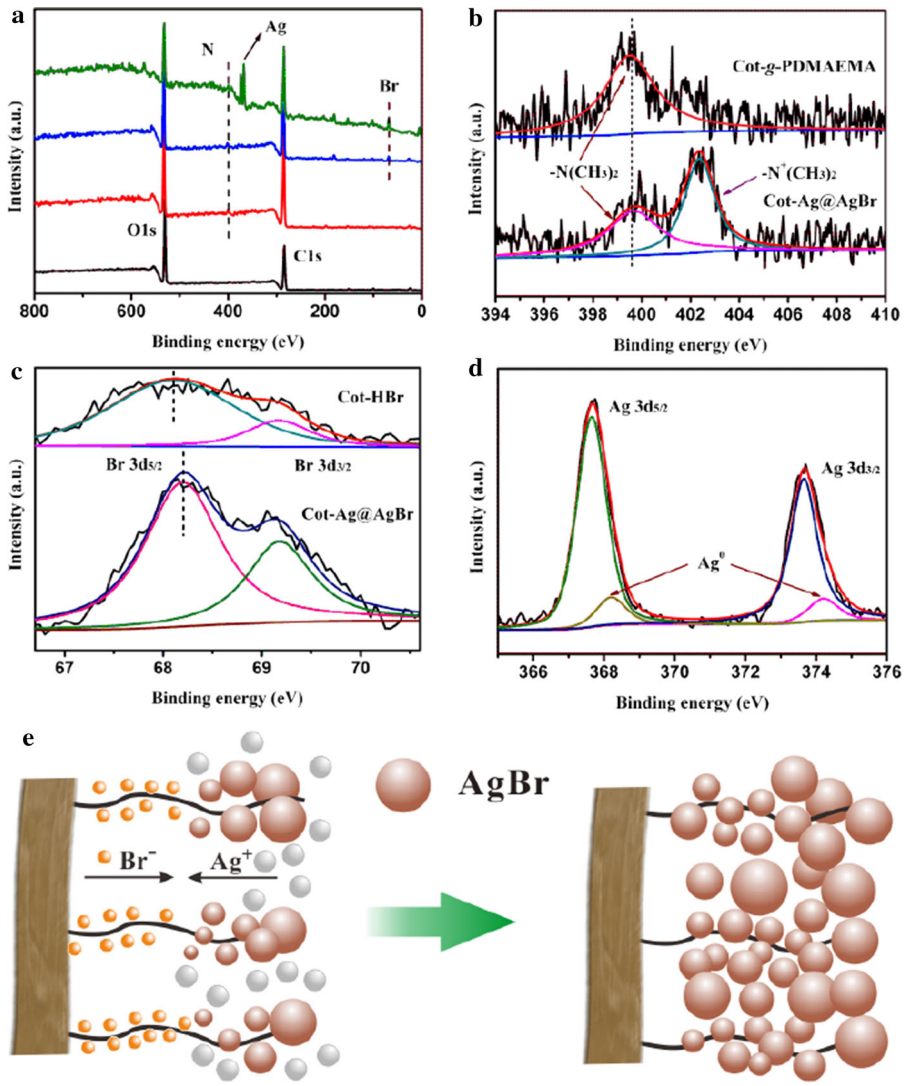

Fig. 3 **a** XPS survey spectra of the pristine cotton fabric, Cot-*g*-PDMAEMA, Cot-HBr, and Cot-Ag@AgBr. **b** N 1 s spectra of the Cot-*g*-PDMAEMA and Cot-Ag@AgBr, **c** Br 3d spectra of the Cot-HBr, and Cot-Ag@AgBr, **d** Ag 3d spectra of the Cot-Ag@AgBr and **e** schematic diagram of AgBr nanocrystal growth

$N^+(CH_3)_2$. The peaks with the binding energies of 68.2 and 69.2 eV in the Br 3d core-level spectra (Fig. 3c) were assigned to Br $3d_{5/2}$ and Br $3d_{3/2}$, respectively and Br $3d_{5/2}$ existed as a primary form (Shahzad et al. 2016). With regard to the spectrum of Br 3d core-level spectra of Cot-Ag@AgBr, the relative contributions of Br $3d_{5/2}$ decreased and Br $3d_{3/2}$ increased, and significant shift of the Br 3d peak was observed, which confirmed the formation of AgBr nanocrystals on the surfaces of the cotton fabric. Owing to the blocking effect of the graft chains, the Br^- peaks of Cot-HBr were less intense than thoes of the Cot-Ag@AgBr. After the introduction of Ag^+ ions, as shown in Fig. 3e, AgBr NPs were in situ formed on the surface of the fabric and the intensity of the Br^- peaks increased owing to the migration of Br^- from the inside toward the outside caused by the reaction between the Ag^+ and Br^- ions. As illustrated in Fig. 3d, the Ag 3d peak was resolved into four peaks at 366.5, 367.5, 372.5, and 373.8 eV. The subpeaks at 366.5 and 372.5 eV could be attributed to the Ag^+, and those at 367.5 eV and 373.8 eV could be ascribed to metallic Ag^0 (Pang and Ge 2017). Based on the intensities of these deconvoluted peaks, the atomic

ratio of Ag/Ag^+ was calculated to be 1:10.5, which indicated that a certain amount of AgBr was reduced to metallic Ag, and consequently suggested that the Ag/AgBr was successfully loaded onto the surface of the cotton fabric.

Photocatalytic degradation performance

The photocatalytic activities of Cot-Ag@AgBr, Ag@ZnO, and as-synthesized Ag@AgBr were investigated under visible light, and RhB was used as the representative organic pollutant. The corresponding degradation curves were obtained by measuring the changes in UV–vis absorbance at 553 nm (RhB) of the residual RhB dye in time for a definite time interval. From Fig. 4a, the intensity of the absorption peak of RhB gradually decreased as the reaction progressed and the peak disappeared completely after 35 min. This confirmed the high catalytic activity of Cot-Ag@AgBr. Before the evaluating the catalytic performance of Cot-Ag@AgBr, it was essential to determine whether the decolorization of the RhB dye was caused by adsorption or not. Figure 4b showed that almost no RhB was removed via adsorption by Cot-Ag@AgBr, illustrating that Cot-Ag@AgBr did not exhibit a strong affinity toward RhB. While Cot-Ag@AgBr exhibited excellent photoactivation ability for the degradation of RhB, it was necessary to compare it with that of a benchmark photodegradation catalyst. Therefore, the Cot-AgBr was used as a reference sample. From Fig. 4b, the degradation rate of Cot-AgBr was only 50% under visible light illumination (350 W) which was much lower than that of Cot-Ag@AgBr, illustrating Ag and AgBr exhibited excellent synergism. At the same dosage of Ag@AgBr, the photodegradation of RhB over Cot-Ag@AgBr and Ag@AgBr was significant. Moreover, the catalytic activity of Cot-Ag@AgBr was lower than Ag@AgBr NPs owing to that the attachment of Ag@AgBr to cotton fabric decrease its lower specific surface area and then fewer active sites. However, Cot-Ag@AgBr can easily separate from the reaction system in practical application and achieve continuous photodegradation of the organic dye. Experiments were also performed to analyze the effectiveness of Cot-Ag@AgBr under sunlight illumination. As illustrated in Fig. 4c, the Cot-Ag@AgBr presented excellent photodegradation activity for RhB and its degradation efficiency was as high as 98% after 8 h of sunlight illumination. The degradation under sunlight illumination required longer time than the process conducted under Xe lamp (350 W) illumination owing to the lower intensity of sunlight compared with that of the Xe lamp.

To quantify the changes in the catalytic activity of different photocatalysts, degradation kinetic parameters were calculated according to (Eq. (2)).

$$-\ln(C/C_0) = kt \quad (2)$$

As shown in Fig. 4d, the degradation kinetic parameter of Cot-Ag@AgBr is 0.074, 3–4 times higher than Cot-AgBr (0.021). The kinetics parameters of Ag@AgBr is 0.129, slightly higher than Cot-Ag@AgBr.

The stability and lifetime of photocatalysts are important parameters because longer life cycles translate into more cost effective catalysts. Thus, Cot-Ag@AgBr was recycled, which showed a reduction in efficiency from 100% (first cycle) to 95% (five cycles) as illustrated in Fig. 4e, This demonstrated its remarkable photocatalytic stability during photodegradation. The slight decrease in degradation rate during recycling was caused by the reduction of the Ag^+ ions (Song et al. 2014). The excellent recyclability of Cot-Ag@AgBr further indicated that the elimination of RhB was predominantly caused by the photodegradation rather than its physical adsorption. The precipitation of Ag^+ not only causes water pollution, but also reduces the catalytic performance of Cot-Ag@AgBr. Subsequently, Ag leaching after photodegradation was analyzed using ICP-AES. The concentration of Ag^+ in the reaction solution was only 21 μg/L, which indicated that the Cot-Ag@AgBr exhibited high durability and photocorrosion resistance.

Other dyes such as methyl orange (MO), methyl blue (MB), congo red (CR), and ofloxacin (OFX) were also tested as typical organic pollutants to further investigate the degradation efficiency of the Cot-Ag@AgBr and the removal rate was provided in Fig. 4f. After a definite interval, removal rates were 92%, 96%, 97%, 99%, and 87% for RhB, MO, MB, CR, and OFX, respectively, illustrating Cot-Ag@AgBr has excellent removal ability for common dyes. To quantify the changes in the catalytic activity of Cot-Ag@AgBr during each cycle of degradation, the degradation kinetic parameters were calculated according to (Eq. (2)) and decreased from 0.074 to

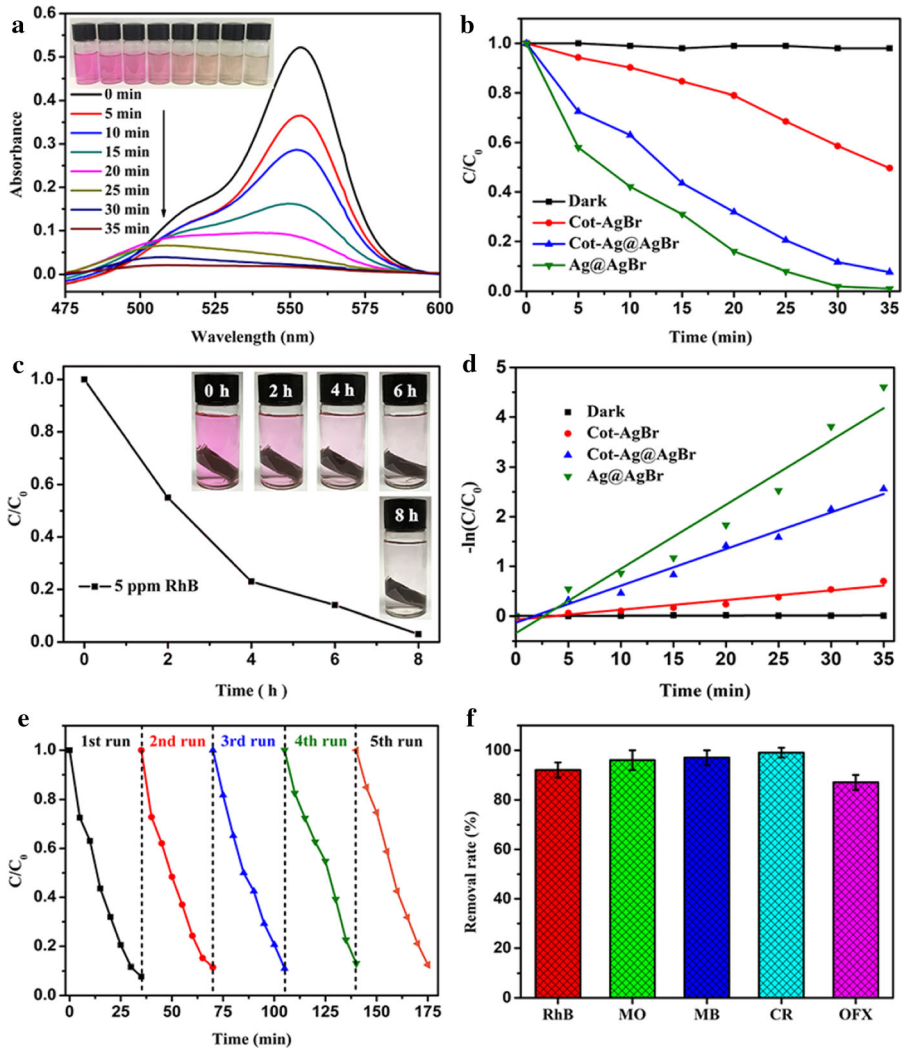

Fig. 4 **a** Time-dependent UV–vis absorption spectra of the RhB solution in the presence of Cot-Ag@AgBr under visible light irradiation (350 W). The insets are photographs of the RhB solutions before and after visible light irradiation for different time intervals; **b** Photodegradation rates of RhB over different photocatalysts; **c** Photocatalytic degradation of RhB (5 ppm) over Cot-Ag@AgBr under the sunlight irradiation. The insets are photographs of color changes of RhB solutions under sunlight radiation (in Shanghai) for different time intervals; **d** Pseudo first order dynamics model of different systems over time; **e** reusability of the Cot-Ag@AgBr for multiple RhB degradation cycles of degradation of RhB under visible light irradiation; **f** photodegradation efficiency of different organic pollutants

0.058 after 5 cycles of usage, illustrating a high catalytic activity retention rate. In addition, comparisons between other reported work and Cot-Ag@AgBr were shown in Table 1. It was demonstrated that the Cot-Ag@AgBr has higher photocatalytic activity and reusability under visible-light irradiation.

Figure 5a illustrates the UV–vis absorption spectra of the pristine and modified cotton fabrics. The pristine cotton fabric, Cot-*g*-PDMAEMA, and Cot-HBr fabrics showed weak absorption peaks in the range of 200–800 nm, illustrating their low light harvesting ability. The absorption range of Cot-Ag@AgBr extended into the visible light range, where a strong peak with a broad shoulder were observed. This confirmed its high catalytic activity under visible light irradiation. The broad absorption peak in the range of 400–550 nm was the characteristic of the Ag NPs (Ansari et al. 2014; Bian et al. 2014; Linic et al. 2011). The surfaces of the Ag NPs could be excited using visible light and electrons could be transferred

Table 1 Comparisons between other reported work and Cot-Ag@AgBr

Photocatalyst	Concentration (mg/L)	Time (min)	Times/last recycle efficiency (%)	Ref.
C-PDA-Ag–WO_3	RB-19 50 mg/L	180	4/85.2	Fan et al. (2019)
rGZn2	MB	60	–	Kumbhakar et al. (2018)
BiOI/SMD-C	RhB 20 mg/L	180	5/95	Zhou et al. (2019)
C/PDA/Ag/AgCl	RB-19 50 mg/L	180	5/89	Ding et al. (2018a, b)
Cot-Ag@AgBr	RhB 10 mg/L	35	5/95	This work

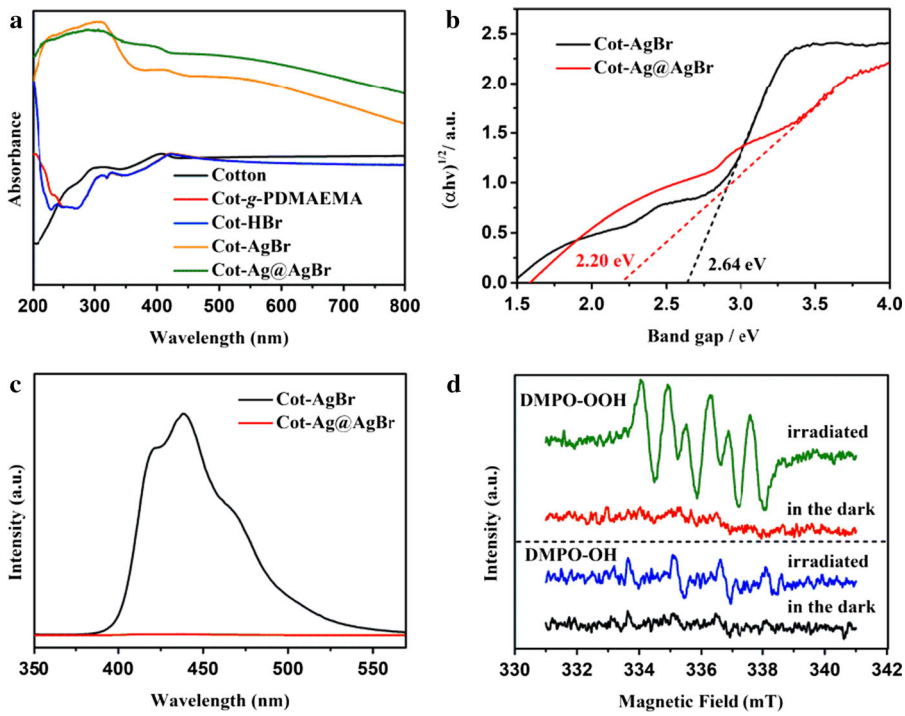

Fig. 5 **a** UV–Vis absorption spectra of pristine cotton fabric, Cot-*g*-PDMAEMA, Cot-HBr, and Cot-Ag@AgBr; **b** Tauc plots of Cot-AgBr and Cot-Ag@AgBr; **c** PL emission spectra of Cot-AgBr and Cot-Ag@AgBr; **d** DMPO spin-trapping EPR spectra of Cot-Ag@AgBr in dark and under visible light irradiation at room temperature

from Ag to AgBr owing to the LSPR; therefore Cot-Ag@AgBr exhibited strong absorption in the visible light region (H. Chen, et al. 2013; Vigderman et al. 2012).

The direct band gap of Cot-AgBr and Cot-Ag@AgBr are calculated from the intercept of the tangent to the plotting $(\alpha h\nu)^2$ versus hν, which had been reported in many literatures (Zhang et al. 2015a, b; Han et al. 2015). From Fig. 5b, the direct band gap of Cot-AgBr and Cot-Ag@AgBr are 2.64 and 2.2 eV, respectively, implying the introduction of Ag atom results in a narrower band gap. The reduction of direct band gap promotes the absorption of visible light, thus improving the photocatalytic efficiency. This can be further elaborated via the analysis of PL spectra.

PL spectra were used to record the electron–hole recombination rate (Fig. 5c). The recombination rate of Cot-Ag@AgBr was significantly lower than that of the Cot-AgBr, demonstrating that the doping of Ag atom suppressed the recombination rate of electron–hole. The causes behind this may be ascribed to that Ag NPs act as electron sinks, and electrons transformed from the conduction band (CB) of the AgBr to

silver, thus inhibiting the recombination of electron–hole.

While Cot-Ag@AgBr appeared to be a promising photocatalyst for the degradation of RhB, it was still important to elucidate the mechanism of RhB degradation over Cot-Ag@AgBr. It is usually believed that the ROS, such as hydroxyl radicals, and superoxide radicals, are generally considered to be the main reactive species during the photocatalytic degradation process. Theefore, it was necessary to identify the types of radical species that dominated the photodegradation process of RhB over Cot-Ag@AgBr under visible light illumination. Consequently, DMPO was selected as the spin trapping for the detection of $\cdot O_2^-$ and ·OH. Figure 5b illustrates the EPR spectra of the $\cdot O_2^-$ and ·OH radicals generated in the presence of Cot-Ag@AgBr at room temperature. No significant EPR signals were observed in ethanol or water systems in the presence of Cot-Ag@AgBr in the dark. After irradiation for 5 min with Xenon lamp irradiation, four weak characteristic signals of ·OH and six strong signals characteristic of the superoxide spin adduct of DMPO (DMPO–OOH) were observed in the water system, which indicated the presence of $\cdot O_2^-$ in the reaction system. The conduction band of AgBr (0.11 eV) cannot reduce O_2 into $\cdot O_2^-$ ($O_2/\cdot O_2^-$, redox potential of −0.33 eV) (Zhao et al. 2017); however, owing to the LSPR of metallic Ag NPs, the surface of polarized Ag could amass electrons, which could be trapped by the dissolved O_2 to form $\cdot O_2^-$. The signals of DMPO–OOH were stronger than those of ·OH for the same illumination time. From the above analysis results, it could be concluded that the $\cdot O_2^-$ rather than the ·OH species played the predominant role during the photodegradation of RhB over Cot-Ag@AgBr.

Evaluation of durability

Fabric-based photocatalysts have irreplaceable advantages, such as facile reusability and excellent adaptivity. However, durability is also an important aspect when evaluating the merits of fabric-based materials. Ultrasonication is a simple and straightforward method for evaluating this property (Lee et al. 2001; Yu et al. 2019). As control experiment, Ag@AgBr NPs were directly deposited on the surface of the pristine cotton fabric, and the obtained sample was denoted as Cot/Ag@AgBr. To study the anchoring effect of graft chains, both Cot-Ag@AgBr and Cot/Ag@AgBr were ultrasonicated for different time intervals. After 2 min of sonication, a large amount of Ag@AgBr NPs (>90%) was peeled off from the surface of Cot/Ag@AgBr, owing to the poor bonding between the functional layer and the substrate. Conversely, as shown in Fig. 6c, no significant leaching of Ag@AgBr NPs was observed (< 2%) after 10 min of sonication treatment, which demonstrated that the Ag@AgBr NPs were firmly immobilized onto the cotton surface. To evaluate the effect of ultrasonication on the photocatalytic efficiency of Cot-Ag@AgBr, samples ultrasonicated for different time intervals were used to degrade fresh RhB solutions. The degradation curves obtained after ultrasonication were virtually identical with that of the pristine Cot-Ag@AgBr fabric, which demonstrated that, even after destructive treatment, Cot-Ag@AgBr could maintain its stability and was still efficient for the photodegradation of RhB. These results also validated the strong immobilization of the Ag@AgBr NPs onto the surface of the cotton fabric. The high interfacial bonding strength could be attributed to the formation of flexible three-dimensional network structures on the surface of the cotton fabric, which trapped the Ag@AgBr NPs during their in situ deposition and could effectively strengthen the attachment of Ag@AgBr NPs to the cotton fabric. Furthermore, SEM images were acquired to analyze the changes in the morphology of Cot-Ag@AgBr after ultrasonication, indicating that the Ag@AgBr NPs were still attached to the surface of the fabric after ultrasonication (Fig. 6a and b). These results indicated that the PDMAEMA graft chains bridge between the Ag@AgBr NPs and cotton fabrics was successful, and could present great potential applications for continuous water purification.

Conclusions

In summary, we demonstrated a novel strategy for fabricating Cot-Ag@AgBr heterogeneous photocatalyst via radiation-induced graft polymerization and the aqueous, one-pot method. The Ag@AgBr NPs were preferably in situ formed on the surface of cotton, owing to the presence of graft chains as the source of bromide ions. Furthermore, Cot-Ag@AgBr combined the remarkable photocatalytic properties of the Ag@AgBr NPs with excellent durability and stability derived from the grafted chains that served as a strong

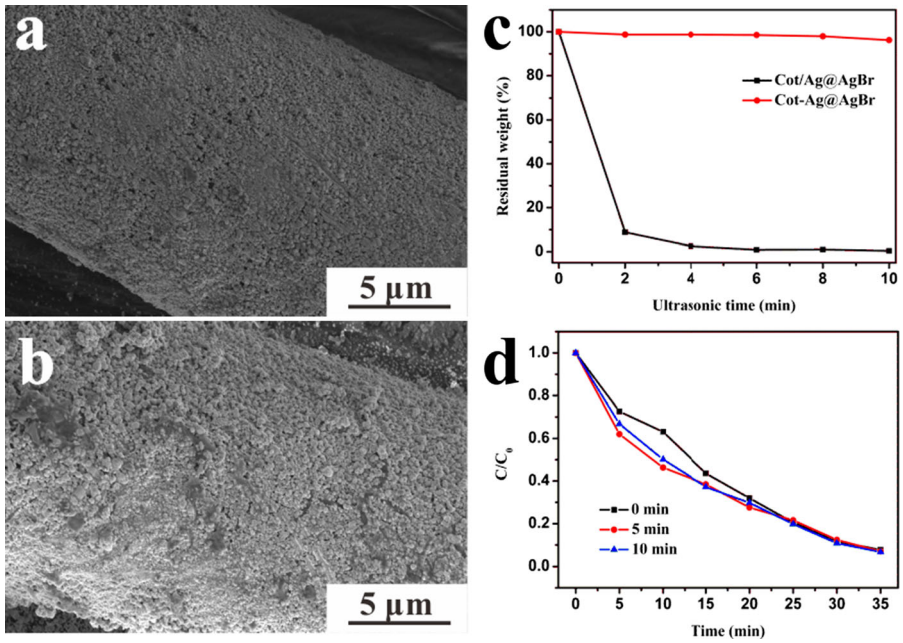

Fig. 6 **a** and **b** SEM images of Cot-Ag@AgBr after ultrasonication for different times; **c** dependence of relative residual weight of Ag/AgBr NPs on ultrasonication time for pristine and modified cotton fabrics; **d** Overlay plots of different ultrasonication time versus photodegradation rate of RhB under visible light irradiation

adhesion layer between the Ag@AgBr NPs and the cotton fabric. The excellent photocatalytic activity was retained after repeated use or even ultrasonic washing for about 10 min. The obtained materials could also completely remove organic pollutants from waste water under sunlight exposure. The EPR experiments demonstrated that the $\cdot O^{2-}$ radical played a more critical role during the photo-degradation process than the ·OH radical. In theory, this process could be expanded as a universal approach for the deposition of semiconductor NPs on a variety of flexible substrates, such as yarns and fibers. Furthermore, this process is believed to be useful for the commercial fabrication of large size semiconductor based flexible photocatalytic materials for water purification.

Acknowledgments We greatly appreciate supports from the National Key R&D Program of China No. 2016YFB0303004, Science Challenge Project, No. TZ2018004, National Natural Science Foundation of China (11305243, 11675247), State Key Laboratory for Modification of Chemical Fibers and Polymer Materials, Donghua University.

References

Ansari SA, Khan MM, Lee J, Cho MH (2014) Highly visible light active Ag@ZnO nanocomposites synthesized by gel-combustion route. J Ind Eng Chem 20(4):1602–1607

Bian Z, Tachikawa T, Zhang P, Fujitsuka M, Majima T (2014) Au/TiO_2 superstructure-based plasmonic photocatalysts exhibiting efficient charge separation and unprecedented activity. J Am Chem Soc 136(1):458–465

Briones RM, Zhuang WQ, Sarmah AK (2018) Biodegradation of metformin and guanylurea by aerobic cultures enriched from sludge. Environ Pollut 243(Pt A):255–262

Chen H, Shao L, Li Q, Wang J (2013) Gold nanorods and their plasmonic properties. Chem Soc Rev 42(7):2679–2724

Chen L, Yang S, Hao B, Ruan J, Ma PC (2015) Preparation of fiber-based plasmonic photocatalyst and its photocatalytic performance under the visible light. Appl Catal B: Environ 166–167:287–294

Cheng D, He M, Ran J, Cai G, Wu J, Wang X (2017) In situ reduction of TiO_2 nanoparticles on cotton fabrics through polydopamine templates for photocatalysis and UV protection. Cellulose 25(2):1413–1424

Ding K, Wang W, Yu D, Wang W, Gao P, Liu B (2018a) Facile formation of flexible Ag/AgCl/polydopamine/cotton fabric composite photocatalysts as an efficient visible-light photocatalysts. Appl Surf Sci 454:101–111

Ding K, Yu D, Wang W, Gao P, Liu B (2018b) Fabrication of multiple hierarchical heterojunction Ag@AgBr/$BiPO_4$/r-GO with enhanced visible-light-driven photocatalytic activities towards dye degradation. Appl Surf Sci 445:39–49

Dong W, Yao Y, Li L, Sun Y, Hua W, Zhuang G, Song W (2017) Three-dimensional interconnected mesoporous anatase TiO_2 exhibiting unique photocatalytic performances. Appl Catal B: Environ 217:293–302

Duan X, Su C, Miao J, Zhong Y, Shao Z, Wang S, Sun H (2018) Insights into perovskite-catalyzed peroxymonosulfate activation: maneuverable cobalt sites for promoted evolution of sulfate radicals. Appl Catal B: Environ 220:626–634

Fan Y, Ma W, Han D, Gan S, Dong X, Niu L (2015) Convenient recycling of 3D AgX/graphene aerogels (X = Br, Cl) for efficient photocatalytic degradation of water pollutants. Adv Mater 27(25):3767–3773

Fan J, Yu D, Wang W, Liu B (2019) The self-assembly and formation mechanism of regenerated cellulose films for photocatalytic degradation of C.I. Reactive Blue 19. Cellulose 26:3955–3972

French (2013) Idealized powder diffraction patterns for cellulose polymorphs. Cellulose 21:885–896

Gao Q, Hu J, Li R, Pang L, Xing Z, Xu L, Wu G (2016) Preparation and characterization of superhydrophobic organic-inorganic hybrid cotton fabrics via gamma-radiation-induced graft polymerization. Carbohydr Polym 149:308–316

Han S, Li J, Yang K, Lin J (2015) Fabrication of a β-Bi_2O_3/BiOI heterojunction and its efficient photocatalysis for organic dye removal. Chin J Catal 36:2119–2126

Hu J, Gao Q, Xu L, Zhang M, Xing Z, Guo X, Wu G (2016) Significant improvement in thermal and UV resistances of UHMWPE Fabric through in situ formation of polysiloxane-TiO_2 hybrid layers. ACS Appl Mater Int 8(35):23311–23320

Hu J, Gao Q, Xu L, Wang M, Zhang M, Zhang K, Wu G (2018) Functionalization of cotton fabrics with highly durable polysiloxane-TiO_2 hybrid layers: potential applications for photo-induced water-oil separation, UV shielding, and self-cleaning. J Mater Chem A 6(14):6085–6095

Huang D, Li J, Zeng G, Xue W, Chen S, Li Z, Cheng M (2019) Facile construction of hierarchical flower-like Z-scheme AgBr/Bi_2WO_6 photocatalysts for effective removal of tetracycline: degradation pathways and mechanism. Chem Eng J 375:121991

Kumbhakar P, Pramanik A, Biswas S, Kole AK, Sarkar R, Kumbhakar P (2018) In-situ synthesis of rGO-ZnO nanocomposite for demonstration of sunlight driven enhanced photocatalytic and self-cleaning of organic dyes and tea stains of cotton fabrics. J Hazard Mater 360:193–203

Lee GS, Lee Y-J, Ha K, Yoon KB (2001) Preparation of flexible zeolite-tethering vegetable fibers. Adv Mater 13:1491–1495

Li B, Wu L, Li L, Seeger S, Zhang J, Wang A (2014) Superwetting double-layer polyester materials for effective removal of both insoluble oils and soluble dyes in water. ACS Appl Mater Int 6(14):11581–11588

Li W, Wang J, He G, Yu L, Noor N, Sun Y, Parkin IP (2017) Enhanced adsorption capacity of ultralong hydrogen titanate nanobelts for antibiotics. J Mater Chem A 5(9):4352–4358

Li P, Guo M, Wang Q, Li Z, Wang C, Chen N, Chen S (2019a) Controllable synthesis of cerium zirconium oxide nanocomposites and their application for photocatalytic degradation of sulfonamides. Appl Catal B: Environ 259:118107

Li X, Qin L, Zhang Y, Xu Z, Tian L, Guo X, Zhang G (2019b) Self-assembly of Mn(II)-amidoximated PAN polymeric beads complex as reusable catalysts for efficient and stable heterogeneous electro-fenton oxidation. ACS Appl Mater Int 11(4):3925–3936

Li Y, Wang S, Chang W, Zhang L, Wu Z, Song S, Xing Y (2019) Preparation and enhanced photocatalytic performance of sulfur doped terminal-methylated g-C_3N_4 nanosheets with extended visible-light response. J Mater Chem A

Liang S, Chang Y, Wang Y, Zhang D, Pu X (2019) Novel one-step combustion synthesis of BiOBr:Yb^{3+}, Er^{3+}/AgBr upconversion heterojunction photocatalysts with enhanced vis/NIR photocatalytic activities. Catal Sci Technol 9(9):2103–2110

Linic S, Christopher P, Ingram DB (2011) Plasmonic-metal nanostructures for efficient conversion of solar to chemical energy. Nat Mater 10:911

Liu S, Peng Y, Chen J, Yan T, Zhang Y, Liu J, Li J (2019) A new insight into adsorption state and mechanism of adsorbates in porous materials. J Hazard Mater 382:121103

Ma X, Wang X, Yu C, Song Y, Liang J, Min Q, Zhang F (2019) Effects of primary nanobuilding blocks on the photocatalytic performance of TiO_2 hierarchical hollow microspheres. J Alloy Compd 773:352–360

Mou H, Song C, Zhou Y, Zhang B, Wang D (2018) Design and synthesis of porous Ag/ZnO nanosheets assemblies as super photocatalysts for enhanced visible-light degradation of 4-nitrophenol and hydrogen evolution. Appl Catal B: Environ 221:565–573

Nakamura K, Nakamura J, Matsumoto K (2019) Filtration and backwashing behaviors of the deep bed filtration using long length poly-propylene fiber filter media. J Taiwan Inst Chem E 94:31–36

Pang Y, Song L, Chen C, Ge L (2017) In situ synthesis of tetrahedron-shaped hollow porous Ag@AgBr plasmonic photocatalysts with highly efficient visible-light performance by a template-assisted method. Appl Surf Sci 420:361–370

Qin S, Qin D, Ford WT, Resasco DE, Herrera JE (2004) Functionalization of single-walled carbon nanotubes with polystyrene via grafting to and grafting from methods. Macromolecules 37(3):468–478

Qin Q, Guo R, Lin S, Jiang S, Lan J, Lai X, Zhang Y (2019) Waste cotton fiber/Bi_2WO_6 composite film for dye removal. Cellulose 26(6):3909–3922

Ran J, Bi S, Jiang H, Telegin F, Bai X, Yang H, Wang X (2019) Core–shell $BiVO_4$@PDA composite photocatalysts on cotton fabrics for highly efficient photodegradation under visible light. Cellulose 26(10):6259–6273

Segal L, Creely JJ, Martin Jr AE, Conrad CM (1959) An enpirical method for estimating the degree of crystallinity of native cellulose using the X-ray diffractometer. Text Res J 786–794

Shahzad A, Yu T, Kim WS (2016) Controlling the morphology and composition of Ag/AgBr hybrid nanostructures and enhancing their visible light induced photocatalytic properties. RSC Adv 6(60):54709–54717

Song J, Lee I, Roh J, Jang J (2014) Fabrication of Ag-coated AgBr nanoparticles and their plasmonic photocatalytic applications. RSC Adv 4(9):4558–4563

Tan B, Gao B, Guo J, Guo X, Long M (2013) A comparison of TiO_2 coated self-cleaning cotton by the sols from peptizing and hydrothermal routes. Surf Coat Technol 232:26–32

Vigderman L, Khanal BP, Zubarev ER (2012) Functional gold nanorods: synthesis, self-assembly, and sensing applications. Adv Mater 24(36):4811–4841

Wang H, Gao J, Guo T, Wang R, Guo L, Liu Y, Li J (2012a) Facile synthesis of AgBr nanoplates with exposed 111 facets and enhanced photocatalytic properties. Chem Commun (Camb) 48(2):275–277

Wang Z, Liu J, Chen W (2012b) Plasmonic Ag/AgBr nanohybrid: synergistic effect of SPR with photographic sensitivity for enhanced photocatalytic activity and stability. Dalton Trans 41(16):4866–4870

Wang Y, Ding X, Chen X, Chen Z, Zheng K, Chen L, Zhang X (2017) Layer-by-layer self-assembly photocatalytic nanocoating on cotton fabrics as easily recycled photocatalyst for degrading gas and liquid pollutants. Cellulose 24(10):4569–4580

Wang M, Zhang M, Pang L, Yang C, Zhang Y, Hu J, Wu G (2019) Fabrication of highly durable polysiloxane-zinc oxide (ZnO) coated polyethylene terephthalate (PET) fabric with improved ultraviolet resistance, hydrophobicity, and thermal resistance. J Colloid Interface Sci 537:91–100

Xiao X, Ge L, Han C, Li Y, Zhao Z, Xin Y, Qiu P (2015) A facile way to synthesize Ag@AgBr cubic cages with efficient visible-light-induced photocatalytic activity. Appl Catal B: Environ 163:564–572

Xu H, Yan J, Xu Y, Song Y, Li H, Xia J, Wan H (2013) Novel visible-light-driven AgX/graphite-like C_3N_4 (X = Br, I) hybrid materials with synergistic photocatalytic activity. Appl Catal B: Environ 129:182–193

Xu P, Yang J, Chen Y, Li Y, Jia X, Song H (2019) Wood-derived fiber/BiOBr/AgBr sponges by in situ synthesis for separation of emulsions and degradation of dyes. Mater Des 183:108179

Yang X, Jiang X, Huang Y, Guo Z, Shao L (2017) Building nanoporous metal-organic frameworks "Armor" on fibers for high-performance composite materials. ACS Appl Mater Int 9(6):5590–5599

Yang R, Dong F, You X, Liu M, Zhong S, Zhang L, Liu B (2019) Facile synthesis and characterization of interface charge transfer heterojunction of Bi_2MoO_6 modified by Ag/AgCl photosensitive material with enhanced photocatalytic activity. Mater Lett 252:272–276

Yu L, Shang X, Chen H, Xiao L, Zhu Y, Fan J (2019) A tightly-bonded and flexible mesoporous zeolite-cotton hybrid hemostat. Nat Commun 10(1):1932

Zhang W, Cao Y, Liu N, Chen Y, Feng L (2014) A novel solution-controlled hydrogel coated mesh for oil/water separation based on monolayer electrostatic self-assembly. RSC Adv 4(93):51404–51410

Zhang C, Shao M, Ning F, Xu S, Li Z, Wei M, Duan X (2015a) Au nanoparticles sensitized ZnO nanorod@nanoplatelet core–shell arrays for enhanced photoelectrochemical water splitting. Nano Energy 12:231–239

Zhang C, Yang HC, Wan LS, Liang HQ, Li H, Xu ZK (2015b) Polydopamine-coated porous substrates as a platform for mineralized beta-FeOOH nanorods with photocatalysis under sunlight. ACS Appl Mater Int 7(21):11567–11574

Zhang M, Gao Q, Yang C, Pang L, Wang H, Li R, Wu G (2017) Preparation of antimicrobial MnO^{4-}-doped nylon-66 fibers with excellent laundering durability. Appl Surf Sci 422:1067–1074

Zhang H, Yu D, Wang W, Gao P, Zhang L, Zhong S, Liu B (2019a) Recyclable and highly efficient photocatalytic fabric of Fe(III)@$BiVO_4$/cotton via thiol-ene click reaction with visible-light response in water. Adv Powder Technol 30:3182–3192

Zhang H, Yu D, Wang W, Gao P, Zhang L, Zhong S, Liu B (2019b) Construction of a novel BON-Br-AgBr heterojunction photocatalysts as a direct Z-scheme system for efficient visible photocatalytic activity. Appl Surf Sci 497:143820

Zhao Y, Lin C, Bi H, Liu Y, Yan Q (2017) Magnetically separable $CuFe_2O_4$/AgBr composite photocatalysts: preparation, characterization, photocatalytic activity and photocatalytic mechanism under visible light. Appl Surf Sci 392:701–707

Zhou P, Lv J, Xu H, Wang X, Sui X, Zhong Y et al (2019) Functionalization of cotton fabric with bismuth oxyiodide nanosheets: applications for photodegrading organic pollutants, UV shielding and self-cleaning. Cellulose 26:2873–2884

Zhu W, Liu X, Tan L, Cui Z, Yang X, Liang Y, Wu S (2019) AgBr nanoparticles in situ growth on 2D MoS_2 nanosheets for rapid bacteria-killing and photodisinfection. ACS Appl Mater Int